Tetrahedron 64 (2008) 11387–11393

Contents lists available at ScienceDirect

Tetrahedron

journal homepage: www.elsevier.com/locate/tet

Metallic nitride endohedral fullerenes: synthesis and electrochemical properties

Manuel N. Chaur, Andreas J. Athans, Luis Echegoyen *

Chemistry Department, Clemson University, Clemson, SC 29634, USA

ARTICLE INFO

Article history:
Received 29 May 2008
Received in revised form 5 August 2008
Accepted 20 August 2008
Available online 27 August 2008

ABSTRACT

Metallic nitride endohedral fullerenes (MNEFs) are one of the most interesting types of metallofullerenes due to their high yields and interesting electronic properties. The synthesis of these compounds allows the encapsulation of different metals inside fullerenes making it possible to combine the properties of the metal with those of the fullerene. Their interesting electrochemical and optical features make them potential candidates for several applications such as molecular electronics, biomedical imaging, non-linear optical devices, and MRI agents. We report herein the synthesis, isolation, and electrochemical properties of the larger MNEFs including $Gd_3N@C_{82}$ and $Gd_3N@C_{86}$, reported here for the first time.

Published by Elsevier Ltd.

1. Introduction

Almost concurrently with the discovery of C_{60} by Smalley and co-workers,[1] endohedral fullerenes were detected in the mass spectra of the soot obtained from vaporization of graphite impregnated with $LaCl_3$.[2] $La@C_{60}$ was detected and further work by Smalley and co-workers using a modified vaporization procedure and La_2O_3 in place of $LaCl_3$, resulted in the synthesis of $La@C_{60}$, $La@C_{70}$, $La@C_{74}$, and $La@C_{82}$.[3]

However, while metal atoms trapped inside of fullerene cages have been known for some time, there had been no reports of trimetallic nitride clusters trapped inside fullerenes until Stevenson and co-workers reported the synthesis and isolation of $Sc_3N@C_{80}$ in 1999.[4] This result was unexpected due to the fact that neither the Sc_3N cluster nor the I_h C_{80} had been prepared individually. However, together they form a very stable compound. It was later determined that this stability was due to the electronic interaction between the cluster and the cage. More specifically, there is a transfer of six electrons from the cluster to the cage. This was postulated by Campanera and co-workers by a combination of density functional theory (DFT) calculations and a re-examination of the crystal structure of Sc_3NC_{80}.[5] Experimental proof of this interaction from EPR studies was obtained by Dinse.[6] Dunsch later published an extensive study on $Sc_3N@C_{80}$ using photoemission and X-ray absorption spectroscopy to determine the electronic structure and conclusively show that there is indeed an electron transfer from the cluster to the cage.[7] Dunsch later performed an EPR study about $Sc_3N@C_{68}$ to further confirm this electronic transfer for cages other than C_{80}.[8] These studies showed that upon both oxidation and reduction the spin density was delocalized on both the cluster and the cage and that MNEFs can be viewed as a cluster donating six electrons from its HOMO to the encapsulating cage's LUMO. This electron transfer can be seen as the general stabilizing force in all MNEFs comprising both IPR (Isolated Pentagon Rule) and non-IPR cages. The stabilization afforded by the transfer of these electrons correlates with the fact that neither the trimetallic nitride clusters nor the encapsulating fullerenes of the same symmetry can be isolated as neutral species by themselves.

The synthesis of MNEFs traditionally was accomplished with the so-called trimetallic nitride template (TNT) method as introduced for the first time by Stevenson and co-workers.[4] However, several other methods have also been used to prepare these types of metallofullerenes. A modification was introduced by Dunsch and co-workers called the reactive gas atmosphere method.[9] Using this method it was possible to prepare gram scale quantities of MNEFs. With the reactive gas atmosphere method, Chaur and co-workers have been able to synthesize many of the larger metallofullerenes, $M_3N@C_{2n}$ (M=Nd, Pr, Ce, and La), and study the electrochemical properties of metallofullerenes larger than $M_3N@C_{80}$.[10]

The redox properties of these compounds have been shown to be highly dependent on the nature of the metallic cluster and on the size of the carbon cage. For instance, $M_3N@C_{2n}$ metallofullerenes exhibit a decrease of their HOMO–LUMO gaps as the carbon cage size increases from C_{80} to C_{88}. Reversible oxidation and reduction waves are observed for $M_3N@C_{88}$ unlike smaller MNEFs.[10]

One of the most interesting features of MNEFs is that different metallic clusters can be encapsulated inside the fullerene cages.[10,11]

* Corresponding author. Tel.: +1 864 656 5030; fax: +1 864 656 6613.
E-mail address: luis@clemson.edu (L. Echegoyen).

0040-4020/$ – see front matter Published by Elsevier Ltd.
doi:10.1016/j.tet.2008.08.060

Exciting to researchers is that these clusters, with metals having magnetic, optically active, highly paramagnetic, and radioactive properties, can be used in many applications in different fields such as molecular electronics and as potential MRI agents.[12] Herein is presented a complete study of the synthesis, isolation, and electrochemical properties of MNEFs including the new gadolinium nitride-based metallofullerenes $Gd_3N@C_{82}$ and $Gd_3N@C_{86}$, reported here for the first time.

2. Synthesis of MNEFs

Stevenson and Dorn prepared MNEFs by using what came to be known as the trimetallic nitride template (TNT) method, where graphite rods packed with Sc_2O_3 were arced under an atmosphere of helium and N_2 as the nitrogen source. While successful, this method has some drawbacks, most notable that it produces a large amount of empty cage fullerenes, mostly C_{60} and C_{70}.[4] Dunsch and co-workers attempted to prepare MNEFs using a solid nitrogen source (calcium cyanamide, CaNCN) packed into the rods during arcing. They were able to prepare $Sc_3N@C_{80}$; however, the yields ranged between 3 and 42%.[9] While they were also able to isolate $Sc_3N@C_{78}$ using this method with decreased amounts of empty cage fullerenes, the low reproducibility of the yields made this method impractical.

Improvement was achieved by Dunsch and co-workers with the introduction of the reactive gas atmosphere method.[9] In this method, the rods were packed as in the TNT method, but instead of N_2 as the source of nitrogen, ammonia (NH_3) gas was introduced as the nitrogen source. Under these conditions MNEFs were produced as the dominant compounds in the soot extracts. Furthermore, the increase in selectivity was such that very low yields (less than 5%) of empty cage fullerenes and non-MNEFs were obtained. This was the first demonstration of a synthesis, which could preferentially produce MNEFs as the major product.

Further advances in the synthesis of MNEFs were made recently by Stevenson. His group was able to improve the yield of $Sc_3N@C_{80}$ and to decrease the amount of empty cage fullerenes using the TNT method combined with what he called the CAPTEAR (Chemically Adjusting Plasma Temperature, Energy, and Reactivity) approach, which involved introducing a solid source of NO_x gas (in this case, $Cu(NO_3)_2 \cdot 2.5H_2O$) in order to 'tune' the temperature and energy of the plasma inside the reactor during the arcing process.[13] In this way, $Sc_3N@C_{80}$ was produced as 96% of the soot extract with the other 4% containing mostly $Sc_3N@C_{78}$ and negligible amounts of empty cages. This is in contrast with the original method of Dorn,[4] which produces $Sc_3N@C_{80}$ as 4% of the soot extract. Stevenson also investigated using copper metal as an additive, arcing rods packed solely with Cu and Sc_2O_3 and containing no graphite, which is usually packed along with the metal oxide.[14] The control experiments, with rods only packed with Sc_2O_3 gave 15% yield of $Sc_3N@C_{80}$ along with 47% C_{60} and 26% C_{70}. The remainder was made up of higher fullerenes such as C_{76}, C_{78}, and C_{84} and $Sc_3N@C_{68}$ and $Sc_3N@C_{78}$. When Cu was added into the rod packing, the yield of MNEFs increased, with the highest % yield occurring at 50 wt % of Cu. Surprisingly, when the Cu packing was increased to 67 wt %, the overall mass of MNEFs extracted was at its maximum. The exact effect of the Cu additive and the reason for this surprising difference is not well understood and is currently under study in Stevenson's laboratories.

3. MNEF families

As mentioned before, Stevenson and co-workers prepared MNEFs with Sc as the metal, most notably $Sc_3N@C_{80}$. They initially reported that the C_{80} cage had I_h symmetry, based on the X-ray crystal structure.[4] However, further investigations uncovered a D_{5h} isomer of $Sc_3N@C_{80}$, characterized by ^{13}C NMR, HPLC, and mass spectroscopy.[15] While Duchamp and co-workers were the first to detect this D_{5h} isomer, Krause and co-workers were the first to isolate it and fully characterize it.[16] This was achieved via HPLC using a linear combination of two columns in order to separate the two isomers. Through a detailed UV–vis/NIR and vibrational spectroscopy study, Krause and co-workers were able to assign D_{5h} symmetry to the newly isolated isomer, corroborating the symmetry proposed by Dorn.[15] These results were surprising given that for the seven possible isomers of C_{80} that obey the isolated pentagon rule (IPR), only two, with D_2 and D_{5d} symmetry, had been isolated as the empty cages.

The discovery of $Sc_3N@C_{80}$ was accompanied by the discoveries of other Sc_3N-containing cages, such as $Sc_3N@C_{68}$, $Sc_3N@C_{70}$, and $Sc_3N@C_{78}$.[17–19] What was surprising about these discoveries was that for $Sc_3N@C_{68}$ and $Sc_3N@C_{70}$, the fullerene cages were isomers that did not obey the IPR. Indeed, for cages C_{70} and smaller, only C_{60} obeys the IPR. Additionally, empty non-IPR cages have never been isolated while it is quite common to isolate their MNEF analogues.

The only other group III metal besides Sc that has formed a MNEF is yttrium, with $Y_3N@C_{80}$ being the most abundant member of the family. Beyond Sc and Y, only lanthanide metals have been shown to form MNEFs. MNEFs have been formed with Sc, Y, Er, Dy, Tb, Ho, Tm, Lu, and Gd.[4,9,20–25] As the size of the metal in the trimetallic nitride cluster inside C_{80} increases, the geometry of the cluster deviates from planarity. While the Sc_3N cluster is completely planar inside C_{80}, the larger metallic clusters are pyramidalized. Dunsch found that the geometry of the Dy_3N cluster was significantly non-planar.[26] The Gd_3N cluster was found to have a pyramidal geometry with the nitrogen atom out of the Gd_3 plane by 0.5 Å.[24] Additionally, Dunsch found that, similar to Dy, Tm, and Tb, cages larger than C_{80} were formed in large enough quantities that they could be isolated and their properties studied.[11] Dunsch postulated that the size of the metal in the cluster dictates the size of the encapsulating cage, and indeed this was borne out since the larger metals produced more quantities of cages larger than C_{80}. However, what was interesting to note was that even the Gd cluster, the largest metal ion reported until recently, preferred the C_{80} cage.[10a]

Surprisingly MNEFs with metals of ionic radii larger than Gd had not been reported until Melin and co-workers arced rods packed with Nd_2O_3 and graphite under the reactive gas atmosphere and obtained $Nd_3N@C_{2n}$ ($40 \leq n \leq 49$) MNEFs. One significant observation is that $Nd_3N@C_{80}$ was the least abundant species formed while $Nd_3N@C_{88}$ was the most abundant. Cages as large as $Nd_3N@C_{98}$ were detected in the mass spectra as well.[10a] For the first time, a cage larger than C_{80} had been formed as the major product (see Fig. 1). This was the first time that significant quantities of an $M_3N@C_{88}$ compound were isolated and its properties studied. In fact, the yield of $Nd_3N@C_{2n}$ (0.2 mg per rod) was found to be greater than that of $Y_3N@C_{2n}$ and $Gd_3N@C_{2n}$ and only slightly less than that of $Sc_3N@C_{2n}$. Thus it appears that while Gd_3N is the upper size limit to stabilize the C_{80} cage, Nd_3N is the lower size limit to stabilize the C_{88} cage.

After Nd, the next two metals of increasing ionic radii size are Pr and Ce and it was found that these metals also preferentially templated the C_{88} cage,[10b] further confirming the hypothesis that Nd was the lower size limit for stabilizing the C_{88} cage. The amount of larger cages was significantly increased, with $M_3N@C_{96}$ being the cage size formed in the second highest amount for Pr and Ce. In fact, Ce shows the amount of $Ce_3N@C_{96}$ to be almost the same as $Ce_3N@C_{88}$. Cages as large as C_{106} were also detected (in the case of the $Ce_3N@C_{2n}$ family) and for the first time no detectable amounts of $Ce_3N@C_{80}$ were formed (see Fig. 2).

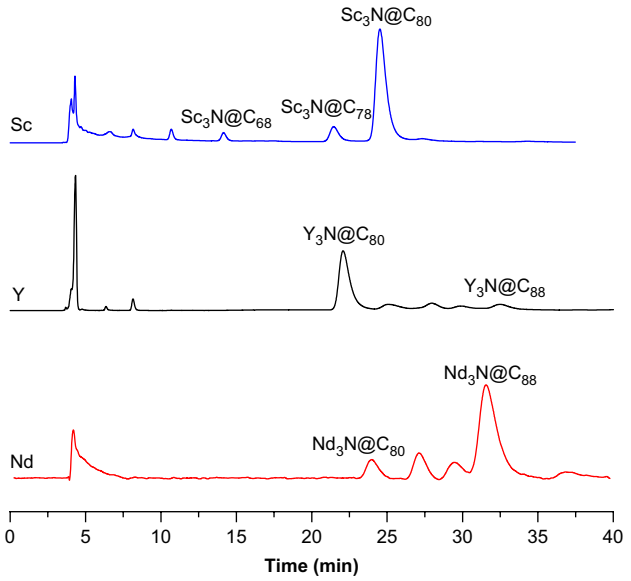

Figure 1. HPLC traces of $Sc_3N@C_{2n}$ (top), $Y_3N@C_{2n}$ (middle), and $Nd_3N@C_{2n}$ clusterfullerene families.

It is also possible to prepare MNEFs containing mixed metal clusters.[17,27] These are prepared by simply packing the graphite rods with a mixture of the desired metal oxides. As may be expected, all statistical stoichiometries in the encapsulated cluster are observed, which increases the number of possible products and complicates the characterization.

4. Isolation and purification of MNEFs

HPLC chromatography has been the traditional method for separation of MNEFs. However, different groups have also used other techniques for their purifications. Dorn's group has taken advantage of the reactivity differences between the empty fullerenes and the various MNEFs formed in the crude soot extract.[28] In particular, they exploited the Diels–Alder reactivity of the various fullerenes in the extract by using a cyclopentadiene-functionalized resin.[28] This method was reversible in that the fullerenes that were

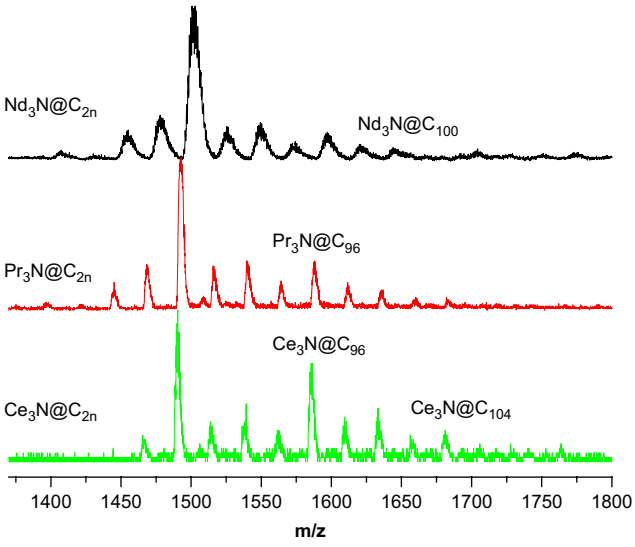

Figure 2. MALDI-TOF mass spectrum of the $Nd_3N@C_{2n}$ (top), $Pr_3N@C_{2n}$ (middle), and $Ce_3N@C_{2n}$ clusterfullerene families.

'trapped' on the resin could be recovered at the end by displacement with maleic anhydride. The empty cage fullerenes and D_{5h} isomer of $M_3N@C_{80}$ all have higher reactivity than the I_h $M_3N@C_{80}$. Thus passing crude soot extract through a column packed with this resin results in the isolation of I_h $M_3N@C_{80}$. Displacement of the other fullerenes from the resin results in their complete recovery. Dorn found that by further controlling the time and temperature, individual empty cage fullerenes could be separated based on reactivity differences with the resin.

Stevenson and co-workers introduced a non-chromatographic 'stir and filter approach' (SAFA) to purify MNEFs, which involves a functionalized diaminosilica.[29] Similar to Dorn's group's exploitation of the reactivity differences of the different fullerenes, Stevenson's group exploited the differences in the amination reactivity in order to selectively isolate MNEFs. Generally, the diaminosilica is added to a xylene solution of crude MNEF soot extract. The mixture is stirred at room temperature and at the end of the reaction period, the mixture is simply filtered. All of the fullerenes except for I_h $M_3N@C_{80}$ are immobilized on the silica and stay behind on the filter. What remains in the xylene filtrate is I_h $M_3N@C_{80}$. While this method is convenient and affords large quantities of isomerically pure I_h $M_3N@C_{80}$, it has the disadvantage of irreversibly immobilizing the other fullerenes on the silica, which so far have not been recovered.

Another method for obtaining isomerically pure I_h $Sc_3N@C_{80}$ involves a selective chemical oxidation approach developed by Elliott and co-workers.[30] This method is based on the pronounced difference in the first oxidation potential between the D_{5h} and I_h isomers, with D_{5h} being easier to oxidize. A chemical oxidant (tris(*p*-bromophenyl)-aminium hexachloroantimonate) with a potential between those of the two isomers was added to a solution of the isomeric mixture. This reaction mixture was then deposited onto a silica gel column and eluted. The oxidant and the oxidized D_{5h} isomer are strongly adsorbed to the column while the unreacted I_h $Sc_3N@C_{80}$ is eluted. The relative purity was determined by electrochemistry. The disadvantage of this method is that the D_{5h} isomer is irreversibly oxidized and trapped on the column and has not, to date, been recovered. Efforts are underway to do so.

The current purification method utilized by Echegoyen's group is HPLC. Typically, crude soot extract is injected onto a Buckyprep-M semi-preparative column in order to determine, which compounds are present. This is coupled with MALDI-TOF mass spectral analysis. Once the constituent MNEFs have been identified, a preparative Buckeyprep-M column and multiple HPLC separations are performed in order to isolate each individual band. The bands are subsequently checked for isomeric purity by injecting into an HPLC with a linear combination of two columns (Buckyprep-M followed by Buckyprep). MNEFs present as only one isomer appear as sharp peaks in the HPLC trace while MNEFs that are present as multiple isomers appear as multiple peaks (these same isomers typically appear as single peaks on the single Buckyprep-M column, emphasizing the importance of this analysis for determining isomeric purity) (see Fig. 3). The purified MNEFs are then characterized by MALDI-TOF, electron dispersion spectroscopy (EDS), electrochemistry, and, when a suitable crystal can be grown, X-ray crystallography.

Figures 3 and 4 show the HPLC chromatogram and MALDI-TOF MS of the $Gd_3N@C_{2n}$ mixture and five isolated fractions including the new $Gd_3N@C_{82}$ and $Gd_3N@C_{86}$, reported here for the first time. These two MNEFs complete the $Gd_3N@C_{2n}$ family and allow the study of the influence of the cage size on the electrochemical properties in MNEFs with the same metallic cluster (Section 6.2). These two MNEFs were also analyzed by EDS (see Fig. 5), observing in each case the characteristic peaks of Gd, confirming the nature of these compounds.

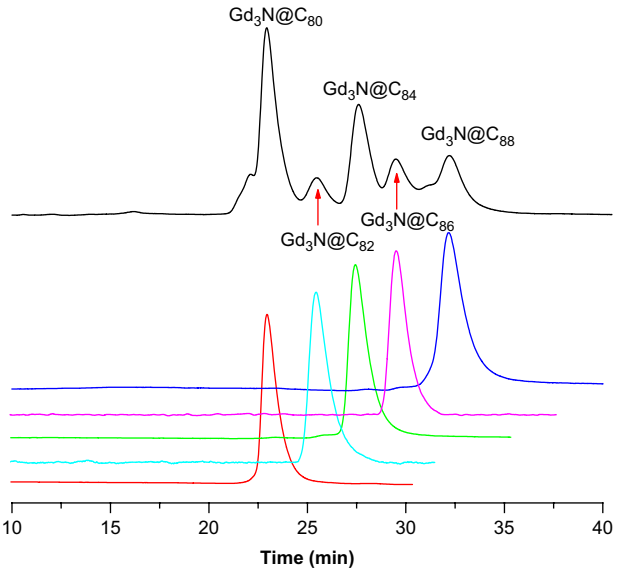

Figure 3. HPLC separation of the $Gd_3N@C_{2n}$ clusterfullerene family. Buckyprep-M column, 4.0 mL/min flow rate of toluene; 372 nm detection.

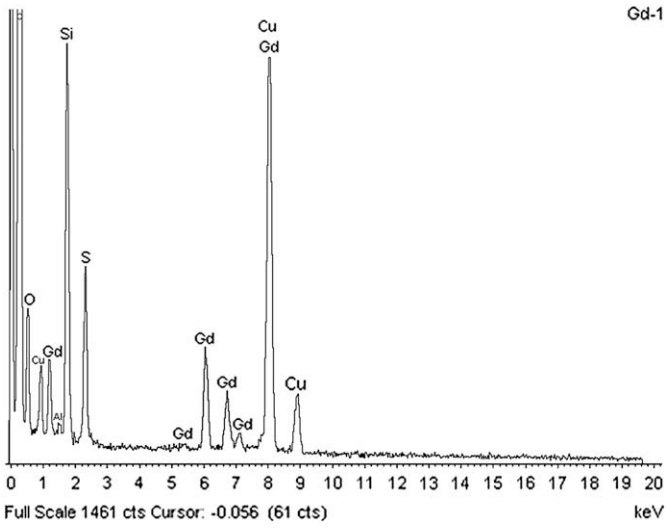

Figure 5. EDS of $Gd_3N@C_{82}$. Copper and aluminum are coming from the grid and sample holder. Sulfur and oxygen are probably coming from the solvents used to manipulate the samples (ether and carbon disulfide). Silicon is appearing as an impurity after passing the sample through a silica column (in a Pasteur pipette) when the CVs were done.

5. Characterization of MNEFs

While MALDI-TOF and HPLC are useful techniques for determining the species present and for measuring purity, more concrete characterization of MNEFs is often very challenging. This is due to the fact that many of the clusters inside the cages are paramagnetic and therefore prevent analysis by more traditional methods, such as NMR spectroscopy. Additionally, since there are no protons on the cages, NMR analysis is limited to ^{13}C NMR, which is problematic as typically very small quantities of MNEFs are formed and the natural abundance of ^{13}C is low. Thus ^{13}C NMR analyses are very difficult if not impossible. Because of this, most researchers in this area have turned to other characterization techniques.

Dunsch and co-workers have shown that IR, UV–vis-NIR, and Raman spectroscopies can be used to identify cage isomers based on the fact that regardless of the encapsulated metal in the trimetallic nitride cluster, the isomers will have the same spectral properties.[11] This has been confirmed by X-ray crystal structures of various MNEFs, which confirm Dunsch's spectroscopic studies. For instance, $Gd_3N@C_{84}$ and $Tb_3N@C_{84}$ show very similar UV–vis-NIR absorptions and optical band gaps (see Table 1). It was later shown that those two MNEFs have the same non-IPR symmetry.[31] Thus, spectroscopy can be used as a diagnostic tool in determining which cage isomers are present. This is especially useful when there are difficulties in obtaining single crystals of suitable quality to obtain an X-ray structure.

One interesting conclusion derived from X-ray crystallography is the discovery that the cage isomer for a particular number of carbons is the same regardless of the metal incorporated in the interior cluster. For example, Zuo and co-workers published in 2006 the structure of an egg-shaped non-IPR $Tb_3N@C_{84}$ metallofullerene, which possessed C_s symmetry and was isomer no. 51365 of the possible 51568 non-IPR cages for a C_{84} cage.[32] Further work showed that for $Tm_3N@C_{84}$ and $Gd_3N@C_{84}$, the same egg-shaped non-IPR isomer, no. 51365, was formed around the cluster.[31] These results showed that the same cage isomers are present for the same fullerene cages irrespective of the encapsulated metal (Fig. 6).

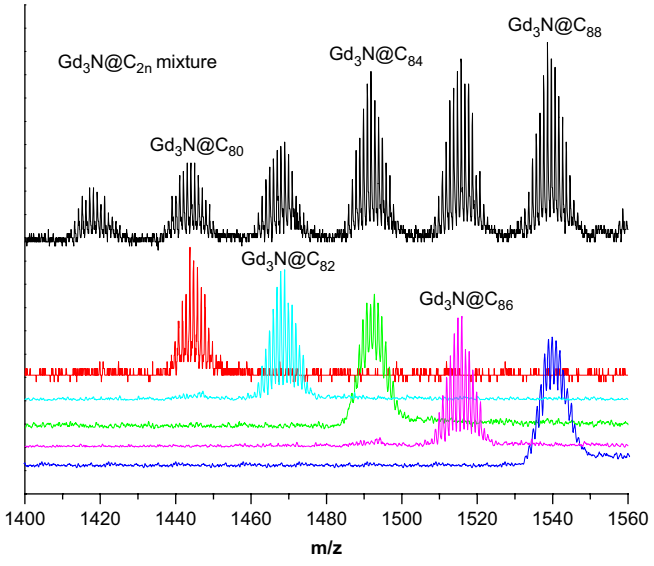

Figure 4. MALDI-TOF MS of the $Gd_3N@C_{2n}$ clusterfullerene family and the isolated fractions.

Table 1
Characteristic UV–vis-NIR absorptions and absorption onset of some $M_3N@C_{2n}$ (n=40, 42, and 44)

TNT EMF	Onset (nm)	Band gap[a] (eV)	UV–vis-NIR absorptions peaks (nm)
$Gd_3N@C_{80}(I)$	780	1.60	407, 555, 675, 705
$Tb_3N@C_{80}(I)$	780	1.60	618, 643, 677, 707
$Dy_3N@C_{80}(I)$	823	1.50	401, 554, 643, 670, 700
$Tm_3N@C_{80}(I)$	780	1.60	407, 540, 675, 705
$Gd_3N@C_{84}$	1375	0.90	378, 493, 626, 1089
$Dy_3N@C_{84}(I)$	1514	0.82	622, 870
$Dy_3N@C_{84}(II)$	1485	0.84	374, 484, 625
$Tb_3N@C_{84}(II)$	—	—	380, 468, 623
$Gd_3N@C_{88}$	1495	0.83	408, 471, 546, 735
$Tb_3N@C_{88}$	—	—	420, 480, 550, 758

[a] Band-gap calculated from the spectral onset (bandgap (eV) ≈ 1240/onset (nm)[20].

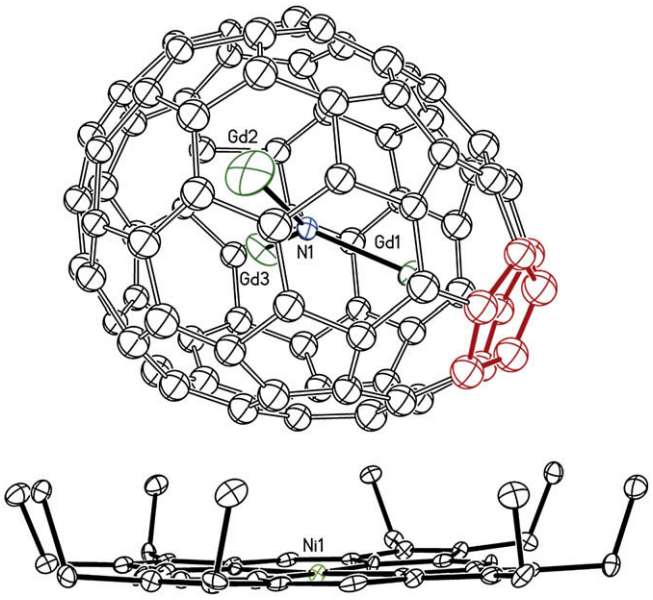

Figure 6. View of the structure of $Gd_3N@C_s(51365)$-C_{84} with 30% thermal contours. The fused pentagons are highlighted in red. Only the major sites for the Gd_3 group are shown. Figure taken from Ref. 31, reproduced by permission of the Royal Society of Chemistry.

6. Electrochemical properties of MNEFs

6.1. Influence of the carbon cage symmetry

Echegoyen and co-workers studied the electrochemical differences between the D_{5h} and I_h isomers of $Sc_3N@C_{80}$.[30] They showed that these two isomers present a pronounced difference in the first oxidation potential and, therefore, they can be electrochemically separated and characterized as described before (see Section 5). This is the first example of the influence of the carbon cage symmetry on the electrochemical properties of MNEFs (see Fig. 7).

6.2. Influence of the carbon cage size

With the isolation of $Gd_3N@C_{82}$ and $Gd_3N@C_{86}$, it is now possible to study for the first time the electrochemical properties of an

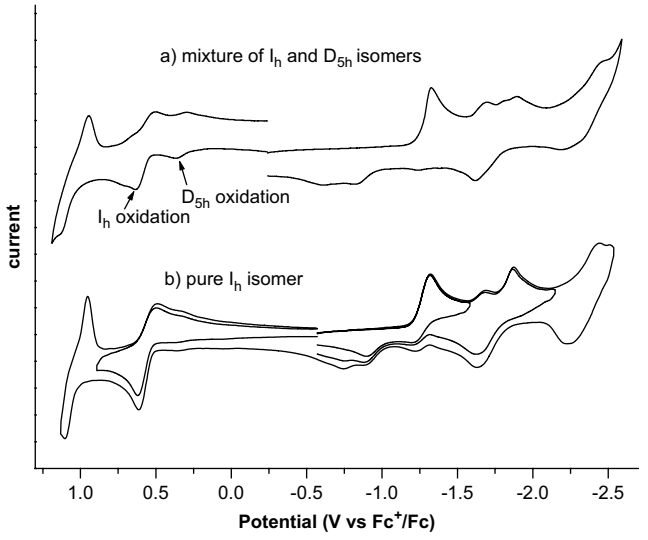

Figure 7. CVs of the mixture of I_h and D_{5h} isomers of $Sc_3N@C_{80}$ (a) and of the pure I_h isomer of $Sc_3N@C_{80}$ (b) obtained in *o*-DCB+0.05 M of $TBAPF_6$ (scan rate 100 mV s^{-1}).

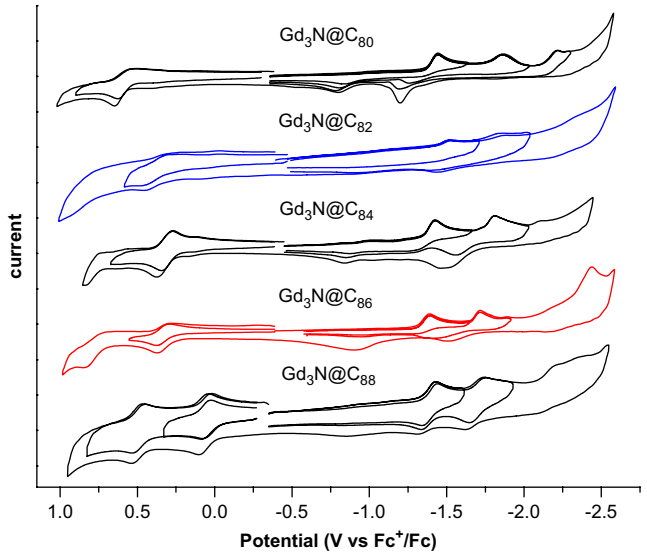

Figure 8. CVs of the $Gd_3N@C_{2n}$ clusterfullerene family obtained in *o*-DCB+0.05 M of $TBAPF_6$ (scan rate 100 mV s^{-1}).

entire family of MNEFs and therefore the cage size influence on the electrochemical potentials.

Figure 8 and Table 2 detail the cyclic voltammograms and redox potentials of the $Gd_3N@C_{2n}$ clusterfullerene family. The first reduction step is roughly the same for the series of $Gd_3N@C_{2n}$ with the exception of $Gd_3N@C_{82}$ where the first reductive potential is shifted cathodically. These compounds exhibit two one-electron reduction processes and a polyelectronic third reduction step. The carbon cage size seems to considerably affect the oxidation process in MNEFs. These metallofullerenes exhibit irreversible oxidation steps that decrease as the carbon cage size increases, therefore, closing the electrochemical band gap. Interestingly $Gd_3N@C_{88}$ exhibits reversible oxidation and reduction waves with the lowest first oxidation potential and HOMO–LUMO gap within the family.

These observations suggest that the LUMO of the MNEF is highly localized on the metallic cluster whereas the HOMO is localized on the carbon cage.

The electrochemical properties of other MNEFs with carbon cages larger than C_{80} have been studied by Chaur and co-workers.[10] The $M_3N@C_{2n}$ (M=Gd, Nd, Pr, and Ce) MNEF families exhibit similar electrochemical trends. As observed for $Gd_3N@C_{2n}$ within a family the first reduction potential stays constant while the first oxidation step decreases as the size of the carbon cage increases.

As expected, $Nd_3N@C_{80}$ and $Pr_3N@C_{80}$ exhibit redox behavior comparable to that of $Sc_3N@C_{80}$, $Er_3N@C_{80}$, $Y_3N@C_{80}$, $Dy_3N@C_{80}$, $Tm_3N@C_{80}$, and $Gd_3N@C_{80}$ described before[10c,33–35] (see Figs. 8–10 and Table 3). At least two irreversible reduction steps and one reversible oxidation potential can be observed.

For the same carbon cage size $M_3N@C_{2n}$ (M=Nd and Pr) exhibit similar electrochemical behavior. Thus, MNEFs show similar

Table 2
Redox potentials (V vs F_c^+/F_c) and electrochemical energy gap $\Delta E_{gap,ec}$ (V) of the $Gd_3N@C_{2n}$ cluster fullerenes in NBu_4PF_6/*o*-DCB

TNT EMF	Redox potential							ΔE_{gap} [V]
	$E_{p,\,red(1)}$	$E_{1/2,\,red(1)}$	$E_{p,\,red(2)}$	$E_{1/2,\,red(2)}$	$E_{p,\,red(3)}$	$E_{1/2,\,ox1}$	$E_{1/2,\,ox2}$	
$Gd_3N@C_{80}$	−1.44		−1.86		−2.15	+0.58		2.02
$Gd_3N@C_{82}$	−1.52		−1.86			+0.37		1.89
$Gd_3N@C_{84}$	−1.37		−1.76			+0.32		1.69
$Gd_3N@C_{86}$	−1.35		−1.70			+0.35		1.70
$Gd_3N@C_{88}$	−1.43	−1.38	−1.74	−1.69		+0.06	+0.49	1.49

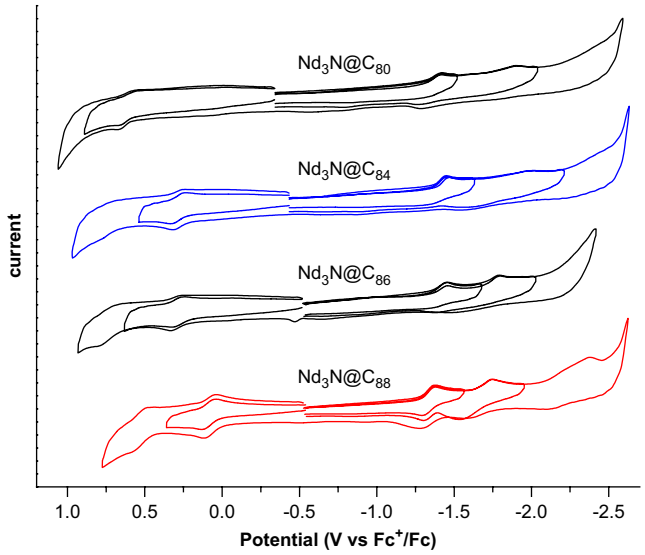

Figure 9. CVs of the $Nd_3N@C_{2n}$ clusterfullerene family obtained in *o*-DCB+0.05 M of $TBAPF_6$ (scan rate 100 mV s^{-1}).

behavior regardless of the nature of the metallic cluster. When going from the C_{80} cage to the C_{86} cage, all of these metallofullerenes exhibit three irreversible reduction steps and at least one reversible oxidation potential.

Besides $Gd_3N@C_{88}$, other MNEFs of the same carbon cage size ($Nd_3N@C_{88}$, $Pr_3N@C_{88}$, and $Ce_3N@C_{88}$) present low HOMO–LUMO gaps and reversible oxidation and reduction steps being this features characteristic of the $M_3N@C_{88}$ metallofullerenes regardless of the encapsulated metal[10] (see Fig. 11).

7. Conclusions and future prospects

Metallic nitride endohedral fullerenes are one of the most fascinating classes of metallofullerenes due to their intrinsic stability (imparted by the electron transfer process that occurs between the metallic cluster and the fullerene cage) and their structures. Even though MNEFs exhibit higher yields than other types of metallofullerenes, further efforts must be made in their preparation and isolation in order to explore their reactivities in detail. Paramagnetic clusters such as Gd_3N, Nd_3N, Pr_3N, and Ce_3N permit MNEFs to be future candidates in applications such as MRI imaging. Their redox behavior allows MNEFs to accept and donate electrons in a reversible way, making them potentially useful in donor–acceptor systems.

Even though their structural variations and the ability to change the metallic cluster are the main features that enable MNEFs to be potentially useful in several fields, there are still numerous questions to be answered, such as the influence of the metallic cluster on the symmetry of the carbon cage or the stabilization that occurs in the different templating stages. Other questions such as the influence of the metallic cluster on the reactivity of the MNEF, the unexplored electrochemical properties of MNEFs larger than $M_3N@C_{88}$, and their symmetries make MNEF research one of the most exciting and dynamic within the fullerene field.

Table 3
Cathodic peak potentials vs F_c^+/F_c of the first reduction step and half wave potential of the other cluster fullerenes isolated, based on Nd and Pr metals

TNT EMF	$E_{p,\ red(1)}$ (V)	$E_{1/2,\ ox(1)}$ (V)	$E_{1/2,\ ox(1)}-E_{p,\ red(1)}$ (V)
$Nd_3N@C_{80}$	−1.42	0.63	2.05
$Pr_3N@C_{80}$	−1.41	0.59	2.00
$Nd_3N@C_{84}$	−1.44	0.31	1.75
$Nd_3N@C_{86}$	−1.46	0.36	1.82
$Pr_3N@C_{86}$	−1.48	0.31	1.78

8. Experimental

8.1. Synthesis of MNEFs

High purity graphite rods (6 mm diameter) purchased from POCO were core-drilled (4 mm diameter) and packed with (3:1), (1:1), and (1:1) mixtures of graphite powder and CeO_2 (cerium oxide), Pr_6O_{11} (praseodymium oxide), and Nd_2O_3 (neodymium oxide), respectively. The rods were annealed at 1000 °C for 12 h and then vaporized in a Krätschmer–Huffman arc reactor under a mixture of ammonia (20 mbar) and helium (200 mbar) using an arc current of 85 A. The soot collected from the arc reactor for each packed rod was extracted with CS_2 in a sonicator for about

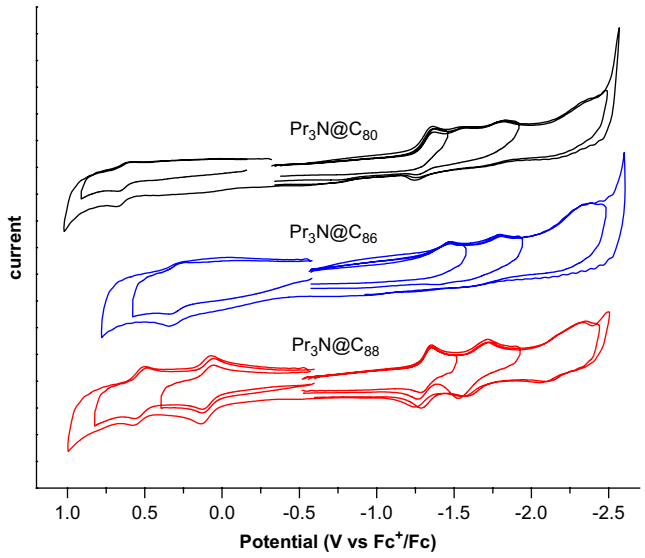

Figure 10. CVs of the $Pr_3N@C_{2n}$ clusterfullerene family obtained in *o*-DCB+0.05 M of $TBAPF_6$ (scan rate 100 mV s^{-1}).

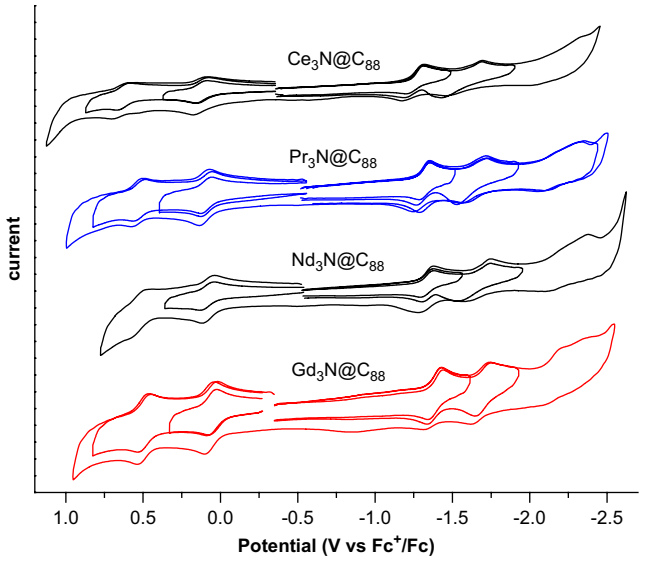

Figure 11. CVs of the $M_3N@C_{88}$ clusterfullerene obtained in *o*-DCB+0.05 M of $TBAPF_6$ (scan rate 100 mV s^{-1}).

2 h. After removal of the solvent, the crude mixtures were washed with ether and acetone until the solution was no longer colored. $Gd_3N@C_{2n}$ metallofullerenes were obtained by extracting all fullerene species from the soot of a standard electric arc reactor via solvent reflux. Empty cage fullerenes were removed from the extract via a Luna Innovations Inc. proprietary chemical subtraction process. A mixture of higher order endohedral metallofullerenes and some $Gd_3N@C_{80}$ was separated from pure $Gd_3N@C_{80}$ via HPLC. The mixture was subsequently used for this study.

8.2. Isolation and identification of MNEFs

The extracted MNEFs were dissolved in toluene and separated by HPLC using a semipreparative 10×250 mm Buckyprep-M column with a flow rate of 4.0 mL/min of toluene. One single HPLC step was necessary for the isolation of $Gd_3N@C_{2n}$ (n=40, 42, and 44), $Nd_3N@C_{2n}$ (n=40, 42, 43, and 44), and $Pr_3N@C_{2n}$ (n=40, 43, and 44). $Gd_3N@C_{2n}$ (n=41 and 43) metallofullerenes were separated in two HPLC steps; in the first step was collected a fraction containing mainly $Gd_3N@C_{82}$ with some $Gd_3N@C_{80}$, and in the second step $Gd_3N@C_{82}$ was isolated pure. For the isolation of $Gd_3N@C_{86}$ it was separated in one step HPLC using a Buckyprep-M column. Then the sample was injected in a linear combination of Buckyprep-M and Buckyprep column with a flow rate of 1.6 mL of toluene per minute. Five fractions were observed, corresponding to different isomers of other Gd-based MNEFs. The main fraction was collected and identified as $Gd_3N@C_{86}$ by mass spectroscopy. All of the isolated fractions were injected onto different HPLC columns (Buckyprep-M and Buckyprep) to ensure their purity. MALDI-TOF mass spectrometry was carried out using a Bruker Omni Flex. For the SEM/EDS analysis, the samples were deposited on TEM grids and the spectra were taken on a HD-2000 STEM, equipped with an Oxford EDS system.

8.3. Electrochemical studies of MNEFs

Cyclic voltammetry was carried out in a one-compartment cell connected to a BAS 100B workstation in a solution of *o*-DCB containing 0.05 M NBu_4PF_6. A 2 mm diameter glassy carbon disk was used as the working electrode. Ferrocene was added to the solution at the end of each experiment as internal standard and all the electrochemical potentials were referenced to its redox couple.

Acknowledgements

We acknowledge financial support from the National Science Foundation A.J.A. and L.E. (Grant number CHE-0509989). This material is based on work supported by the National Science Foundation while L.E. was working there. This material is also based on work supported by Luna Innovations and the Air Force Office of Scientific Research (AFOSR) under contract no. FA9550-06-C-0010. All opinions, findings, conclusions, or recommendations expressed herein are those of the authors and do not necessarily reflect the views of the National Science Foundation. Finally, we would like to thank Luna Innovations for supplying us with the raw $Gd_3N@C_{2n}$ extract from which we separated the $Gd_3N@C_{2n}$ MNEFs.

References and notes

1. Kroto, H. W.; Heath, J. R.; O'Brien, S. C.; Curl, R. F.; Smalley, R. E. *Nature* **1985**, *318*, 162–163.
2. Heath, J. R.; O'Brien, S. C.; Zhang, Q.; Liu, Y.; Curl, R. F.; Kroto, H. W.; Tittel, F. K.; Smalley, R. E. *J. Am. Chem. Soc.* **1985**, *107*, 7779–7780.
3. Chai, Y.; Guo, T.; Jin, C.; Haufler, R. E.; Chibante, L. P. F.; Fure, J.; Wang, L.; Alford, J. M.; Smalley, R. E. *J. Phys. Chem.* **1991**, *95*, 7564–7568.
4. Stevenson, S.; Rice, G.; Glass, T.; Harich, K.; Cromer, F.; Jordan, M. R.; Craft, J.; Hadju, E.; Bible, R.; Olmstead, M. M.; Maitra, K.; Fisher, A. J.; Balch, A. L.; Dorn, H. C. *Nature* **1999**, *401*, 55–57.
5. Campanera, J. M.; Bo, C.; Olmstead, M. M.; Balch, A. L.; Pobelt, J. M. *J. Phys. Chem. A* **2002**, *106*, 12356–12364.
6. Jakes, P.; Dinse, K.-P. *J. Am. Chem. Soc.* **2001**, *123*, 8854–8855.
7. Alvarez, L.; Pichler, T.; Goergi, P.; Schwieger, T.; Peisert, H.; Dunsch, L.; Hu, Z.; Knupfer, M.; Fink, J.; Bressler, P.; Mast, M.; Golden, M. S. *Phys. Rev. B* **2002**, *66*, 035107–035107-7.
8. Yang, S.; Rapta, P.; Dunsch, L. *Chem. Commun.* **2007**, 189–191.
9. Dunsch, L.; Krause, M.; Noack, J.; Georgi, P. *J. Phys. Chem. Solids* **2004**, *65*, 309–315.
10. (a) Melin, F.; Chaur, M. N.; Engmann, S.; Elliott, B.; Kumbhar, A.; Athans, A. J.; Echegoyen, L. *Angew. Chem., Int. Ed.* **2007**, *46*, 9032–9035; (b) Chaur, M. N.; Melin, F.; Elliott, B.; Kumbhar, A.; Athans, A. J.; Echegoyen, L. *Chem.—Eur. J.* **2008**, *14*, 4594–4599; (c) Chaur, M. N.; Melin, F.; Elliott, B.; Athans, A. J.; Walker, K.; Holloway, B. C.; Echegoyen, L. *J. Am. Chem. Soc.* **2007**, *129*, 14826–14829.
11. Dunsch, L.; Yang, S. *Small* **2007**, *3*, 1298–1320.
12. (a) Mikawa, M.; Kato, H.; Okumura, M.; Narataki, M.; Kanazawa, Y.; Miwa, N.; Shinohara, H. *Bioconjugate Chem.* **2001**, *12*, 510–514; (b) Kato, H.; Kanazawa, Y.; Okumura, M.; Taninaka, A.; Yokawa, T.; Shinohara, H. *J. Am. Chem. Soc.* **2003**, *125*, 4391–4397.
13. Stevenson, S.; Thompson, M. C.; Coumbe, H. L.; Mackey, M. A.; Coumbe, C. E.; Phillips, J. P. *J. Am. Chem. Soc.* **2007**, *129*, 16257–16262.
14. Stevenson, S.; Mackey, M. A.; Thompson, M. C.; Coumbe, H. L.; Madasu, P. K.; Coumbe, C. E.; Phillips, J. P. *Chem. Commun.* **2007**, 4263–4265.
15. Duchamp, J. C.; Demortier, A.; Fletcher, K. R.; Dorn, D.; Iezzi, E. B.; Glass, T.; Dorn, H. C. *Chem. Phys. Lett.* **2003**, *375*, 655–659.
16. Krause, M.; Dunsch, L. *ChemPhysChem* **2004**, *5*, 1445–1449.
17. Stevenson, S.; Fowler, P. W.; Heine, T.; Duchamp, J. C.; Rice, G.; Glass, T.; Harich, K.; Hajdu, E.; Bible, R.; Dorn, H. C. *Nature* **2000**, *408*, 427–428.
18. Olmstead, M. M.; de Bettencourt-Dias, A.; Duchamp, J. C.; Stevenson, S.; Marciu, D.; Dorn, H. C.; Balch, A. L. *Angew. Chem., Int. Ed.* **2001**, *40*, 1223–1225.
19. Yang, S.; Popov, A. A.; Dunsch, L. *Angew. Chem., Int. Ed.* **2007**, *46*, 1256–1259.
20. Yang, S.; Dunsch, L. *J. Phys. Chem. B* **2005**, *109*, 12320–12328.
21. Krause, M.; Wong, J.; Dunsch, L. *Chem.—Eur. J.* **2005**, *11*, 706–711.
22. Zuo, T.; Beavers, C. M.; Duchamp, J. C.; Campbell, A.; Dorn, H. C.; Olmstead, M. M.; Balch, A. L. *J. Am. Chem. Soc.* **2007**, *129*, 2035–2043.
23. Lezzi, E. B.; Duchamp, J. C.; Fletcher, K. R.; Glass, T. E.; Dorn, H. C. *Nano. Lett.* **2002**, *2*, 1187–1190.
24. Stevenson, S.; Phillips, J. P.; Reid, J. E.; Olmstead, M. M.; Rath, S. P.; Balch, A. *Chem. Commun.* **2004**, 2814–2815.
25. Krause, M.; Dunsch, L. *Angew. Chem., Int. Ed.* **2005**, *44*, 1557–1560.
26. Yang, S.; Troyanoc, S. I.; Popov, A. A.; Krause, M.; Dunsch, L. *J. Am. Chem. Soc.* **2006**, *128*, 16733–16739.
27. (a) Olmstead, M. M.; de Bettencourt-Dias, J. C.; Duchamp, S.; Stevenson, H. C.; Dorn, A.; Balch, A. L. *J. Am. Chem. Soc.* **2000**, *122*, 12220–12226; (b) Yang, S.; Kalbac, M.; Popov, A.; Dunsch, L. *ChemPhysChem* **2006**, *7*, 1990–1995; (c) Yang, S.; Popov, A. A.; Dunsch, L. *J. Phys. Chem. B* **2007**, *111*, 13659–13663; (d) Chen, N.; Zhang, E.; Wang, C. *J. Phys. Chem. B* **2006**, *110*, 13322–13325; (e) Wang, X.; Zuo, T.; Olmstead, M. M.; Duchamp, J. C.; Glass, T. E.; Cromer, F.; Balch, A. L.; Dorn, H. C. *J. Am. Chem. Soc.* **2006**, *128*, 8884–8889; (f) Chen, N.; Fan, L.; Tai, K.; Wu, Y.; Shu, C.; Lu, X.; Wang, C. *J. Phys. Chem. C* **2007**, *111*, 11823–11828.
28. Ge, Z.; Duchamp, J. C.; Cai, T.; Gibson, H. W.; Dorn, H. C. *J. Am. Chem. Soc.* **2005**, *127*, 16292–16298.
29. (a) Stevenson, S.; Harich, K.; Yu, H.; Stephen, R. R.; Heaps, D.; Coumbe, C.; Philips, J. P. *J. Am. Chem. Soc.* **2006**, *128*, 8829–8835; (b) Stevenson, S.; Mackey, M. A.; Coumbe, C. E.; Philips, J. P.; Elliott, B.; Echegoyen, L. *J. Am. Chem. Soc.* **2007**, *129*, 6072–6073.
30. Elliott, B.; Yu, L.; Echegoyen, L. *J. Am. Chem. Soc.* **2005**, *127*, 10885–10888.
31. Zuo, T.; Walker, K.; Olmstead, M. M.; Melin, F.; Holloway, B. C.; Echegoyen, L.; Dorn, H. C.; Chaur, M. N.; Chancellor, C. J.; Beavers, C. M.; Balch, A. L.; Athans, A. J. *Chem. Commun.* **2008**, 1067–1069.
32. Beavers, C. M.; Zuo, T.; Duchamp, J. C.; Harich, K.; Dorn, H. C.; Olmstead, M. M.; Balch, A. L. *J. Am. Chem. Soc.* **2006**, *128*, 11352–11353.
33. Krause, M.; Liu, X.; Wong, J.; Pichler, T.; Knupfer, M.; Dunsch, L. *J. Phys. Chem. A* **2005**, *109*, 7088–7093.
34. Yang, S.; Zalibera, M.; Rapta, P.; Dunsch, L. *Chem.—Eur. J.* **2006**, *12*, 7848–7855.
35. Cardona, C. M.; Elliott, B.; Echegoyen, L. *J. Am. Chem. Soc.* **2006**, *128*, 6480–6485.